A Recombinant Fusion Protein Immunotherapy Utilizing a Modified Chlorotoxin Molecule Binds Murine Glioblastoma and T cells *In Vitro*

by

Braeden S. Schaefer

A Thesis Presented in Partial Fulfillment
of the Requirements for the Degree
Master of Science

Approved November 2021 by the
Graduate Supervisory Committee:

Tsafrir Mor, Chair
Hugh Mason
Joseph Blattman

ARIZONA STATE UNIVERSITY

December 2021

ABSTRACT

The growing field of immunotherapy has generated numerous promising disease treatment platforms in recent years. By utilizing the innate capabilities of the immune system, these treatments have provided a unique, simplistic approach to targeting and eliminating cancer. Among these, the bispecific T cell engager (BiTE®) model has demonstrated potential as a treatment capable of bringing immune cells into contact with cancer cells of interest and initiating perforin/granzyme-mediated cell death of the tumor. While standard BiTE platforms rely on targeting a tumor-specific receptor via its complementary antibody, no such universal receptor has been reported for glioblastoma (GBM), the most common and aggressive primary brain tumor which boasts a median survival of only 15 months. In addition to its dismal prognosis, GBM deploys several immune-evasion tactics that further complicate treatment and make targeted therapy difficult. However, it has been reported that chlorotoxin, a 36-amino acid peptide found in the venom of *Leiurus quinquestriatus*, binds specifically to glioma cells while not binding healthy tissue in humans. This specificity positions chlorotoxin as a prime candidate to act as a GBM-targeting moiety as one half of an immunotherapeutic treatment platform resembling the BiTE design which I describe here. Named ACDClxΔ15, this fusion protein tethers a truncated chlorotoxin molecule to the variable region of a monoclonal antibody targeted to CD3ε on both CD8+ and CD4+ T cells and is theorized to bring T cells into contact with GBM in order to stimulate an artificial immune response against the tumor. Here I describe the design and production of ACDClxΔ15 and test its ability to bind and activate T lymphocytes against murine GBM *in vitro*. ACDClxΔ15 was shown to bind both GBM and T cells without binding healthy cells *in vitro* but did not demonstrate the ability to activate T cells in the presence of GBM.

DEDICATION

Dedicated to Katie, Cosmo, and Juno – my closest friends.

ACKNOWLEDGEMENTS

Dr. Rebecca Cook, my long-time mentor and the original creator of this project, for giving me my start in research as an 18-year-old that had no idea what they were getting into. A talented scientist and teacher, your creativity and dedication in your approach to science is unmatched. I hope that one day this project meets its lofty expectations, not for my sake, but for yours. Long live ACDClx!

Dr. Mor, for bringing me into your lab and being unbelievably supportive of not only this project, but of myself as well. For providing your expertise, blunt honesty, and unique perspectives. And most of all, for letting me make my own mistakes and learn from them. These experiences have been invaluable in my development as an independent scientist.

Dr. Mason, for welcoming me into your lab and lending your time to this project, and for offering your own unique expertise to explore avenues within this project that otherwise may not have been considered. I greatly appreciate your calm and thoughtful approach to science, which comes as a welcome change of pace in an otherwise often chaotic environment.

Dr. Blattman, for providing the immunological expertise that I so lack, and for offering to assist with this project without hesitation – your help has greatly benefitted this project's trajectory and cannot be discounted.

Members of the Mor and Mason labs alike, past and present, for being the community that makes science so enjoyable. You have all provided your own insights into this project and have helped me immensely over the years, but most importantly, you have saved my sanity by providing a breath of fresh air away from the stress of research on numerous occasions. Special thanks to Michelle, Aya, Joe, Andy, Mary, and Brandon.

Ben Gonzalez, Dr. Debra P. Baluch, and Adam Kindelin, for offering your time and resources to collaborate on some of the most exciting experiments performed for this project. I can't thank you enough for all the things I've learned throughout the process and hope I'm able to return the favor.

Mom, for being selfless and always putting us kids first before yourself, and dad, for always supporting me – you guys mean the world to me.

Finally, the Graduate and Professional Student Association at ASU, for providing partial funding for this project.

TABLE OF CONTENTS

Page

LIST OF TABLES

Table Page

LIST OF FIGURES

Figure Page

1. INTRODUCTION

1.1 *Clinical Significance of Glioblastoma*

Glioblastoma multiforme (GBM) is the most common and aggressive primary brain tumor and the second most common cancer of the central nervous system (CNS), comprising 15% of all intracranial neoplasms and 60-75% of tumors of astrocytic origin [1,2]. GBM can arise as either a primary or secondary tumor, both of which exhibit high heterogeneity. Primary GBM typically occurs spontaneously as a grade IV astrocytoma in the white matter of the brain and can grow rapidly before patients experience symptoms, leading to late detection of the tumor and a less favorable prognosis. Conversely, secondary GBM tumors arise from lower-grade astrocytomas (grades I-III) and grow much slower, leading to a slight increase in post-detection survival time. While GBM arises and metastasizes primarily within the brain, reports of tumor spread to the spinal cord through the cerebrospinal fluid (CSF) have been recorded, though these instances are very rare [3].

Minimal progress has been made in regard to treatment strategies for GBM over the past three decades. The current standard of care – a combination of surgical resection, chemotherapy, and radiotherapy – is employed more so to prolong patient survival rather than to eliminate the tumor entirely, as even in cases of maximum treatment, GBM typically recurs [4]. While these treatments do increase median survival from 3 months to 12-15 months following diagnosis, 5-year survival remains a dismal 3-7% [5]. The aggressively metastatic nature of GBM in combination with its current, inadequate treatment strategy leads to tumor recurrence, and eventually death, in nearly 100% of patients.

1.2 *Barriers to GBM Treatment*

The poor prognosis of GBM is aided by numerous obstacles that stand in the way of its treatment, obstacles that the current standard of care often cannot overcome. These include but are not limited to: (1) metastatic infiltration of GBM within the brain, (2) protection from the blood-brain barrier (BBB), and (3) immune evasion tactics employed within the tumor microenvironment. Identifying and understanding these barriers to treatment in the context of the current care model provides useful insight that can be used to inform the development of more successful therapies for GBM going forward.

The foremost barrier to treatment of GBM involves the tumor's aggressive, metastatic nature. Infiltration of GBM cells throughout the brain gives rise to complications pertaining to complete surgical removal of the tumor, as small populations of malignant cells capable of forming recurrent, satellite tumors often go undetected and thus are not removed during surgery. Surgery is likewise complicated by the location of the tumor, where complete resection of the tumor without removing healthy brain tissue becomes a difficult and dangerous task. As a result, surgical resection cannot be relied upon for complete removal of the tumor, and especially for satellite tumors that may form from small populations of infiltrative cells throughout the brain. Elimination of the complete tumor without harming healthy brain tissue is also a cause of concern for treatment via chemotherapy and radiotherapy, which are typically employed following initial resection to attempt to eliminate any remaining cell populations. While these treatments can slow recurrent tumor progression, the heterogeneity of GBM and the presence of cancer stem cells that up-regulate responses to DNA damage often result in resistance against these therapies [6]. Due to the high rate of GBM recurrence and the ability of small populations of infiltrative cells to give

rise to new satellite tumors, it is pertinent that any effective treatment is capable of eliminating 100% of GBM cells but not healthy tissue.

Another obstacle standing in the way of GBM treatment lies in its protection provided by the blood-brain barrier, a filtering mechanism of brain vasculature that prevents the passage of certain potentially harmful molecules, and often therapeutic drugs, into the brain. Of these excluded molecules, >98% of chemotherapeutics are denied entry, leading to questions regarding the efficacy of chemotherapy in the context of GBM treatment [7]. The most convincing case for chemotherapy thus far showed that combined treatment with radiation therapy increased the median survival of patients versus those receiving radiation alone; however, this resulted in an increase of only 2.5 months (14.6 vs. 12.1 months, respectively) [8]. These observations inform yet another necessary element of an effective therapeutic designed for GBM: it must be able to cross the BBB.

The final barrier to treating GBM discussed here involves its ability to evade the host immune response and induce immunosuppression within the tumor microenvironment. Specifically, GBM prevents antigen-presenting cells (APCs) from activating the anti-tumor immune response by blocking their transport to the lymph nodes through the secretion of cytokines TGF-β and IL-10 [9]. These cytokines also act to induce T regulatory cells (Tregs) and suppress T cell activation, respectively. Induction of Tregs aids in immune evasion by inhibiting and causing exhaustion of cytotoxic CD8+ T cells, adding to the limitation of anti-tumor activity by the immune system [10]. GBM is also known to down-regulate expression of MHC Class I and II receptors on the cell surface, preventing recognition from CD8+ T cells which would normally initiate perforin-granzyme mediated apoptosis against the tumor [11]. Current treatment strategies also contribute to GBM's ability to evade the immune response. Temozolomide

(TMZ), the only chemotherapeutic drug currently approved for treatment of GBM, is known to induce immunosuppression in patients at the doses currently utilized [12]. Combined, these efforts result in an overall reduction in immune-mediated cytotoxic activity against GBM and strongly suggest that an effective treatment should be capable of activating an anti-tumor immune response.

1.3 *Immunotherapy for GBM*

The growing field of immunotherapy stands as one of the most promising alternatives to the current standard of care for GBM. Intended to utilize and stimulate the immune system against disease, emerging immunotherapeutic strategies offer the specificity required to target and eliminate GBM in ways that the current standard of care cannot. This specificity allows for the targeting and elimination of populations of cells that may survive first-line treatments, thereby preventing infiltration and formation of satellite tumors. In addition, these therapies aim to prevent off-target toxicity associated with current treatment options by targeting only the cancer cells of interest and not healthy tissue. Recent attempts at designing immunotherapies for GBM have been encouraging but largely disappointing, due in part to the lack of known universal targets for GBM and the tumor's heterogeneity. The most notable target of attempted GBM immunotherapies is a mutation of the epidermal growth factor receptor (EGFR) known as EGFRvIII, which is expressed by >75% of GBM cells in 30% of patients [13]. This variant was the target of an early peptide vaccine designed to initiate an immune response against the tumor through the creation of antibodies against the mutated receptor [14]. Despite a marked increase in median survival among patients in early stages of clinical trials, the vaccine ultimately failed; biopsies of patients also showed decreased expression of EGFRvIII, suggesting the potential for treatment resistance. Despite this, EGFRvIII remained the most promising target for novel GBM treatments

and has been targeted by many immunotherapeutic platforms, including the bispecific T cell engager (BiTE™) model.

Originally proposed in 1985 as a method to promote T cell-mediated destruction of target cells, BiTEs consist of two single-chain variable fragments (scFvs) of antibodies which are tethered together by a short, inert linker to form a fusion protein (Figure 1) [15]. These antibodies are intended to bring T cells into contact with, and eliminate, specific target cells through targeted antibody binding. The target specificity of a BiTE comes from its antigen-specific antibody fragment, which binds selectively to a target molecule on the cell of interest. The other half of the BiTE consists of an scFv that binds T cells via the T cell receptor (TCR) protein CD3ε, where binding leads to structural changes and eventual signal transduction to induce sustained activation of T cells when the target cell is also bound by its complementary antibody [16]. This method of inducing T cell activation is notable in that it does not require recognition by the major histocompatibility complex (MHC), allowing for T cell-mediated elimination of target cells regardless of TCR specificity. Additionally, it overcomes the problem of MHC-downregulation by cells such as GBM which are known to do so in order to evade the immune response. Unfortunately, the lack of a universal target poses a challenge in the creation of a successful BiTE for GBM. The most prominent BiTE for GBM did demonstrate the ability to cross the BBB, but once again targeted EGFRvIII with little success due to the lack of homogenous expression throughout the tumor and the resulting treatment resistance caused by rapid expansion of EGFRvIII-negative cells [17]. While the ability of these treatments to effectively establish an anti-tumor immune response against EGFRvIII-positive cells is encouraging, it is clear that development of a curative treatment depends largely on the presence of a universal target for GBM.

1.4 *Chlorotoxin*

Nearly 20 years ago, researchers in the Sontheimer lab were studying chlorotoxin, a 36-amino acid peptide found in the venom of the deathstalker scorpion (*L. quinquestriatus*), when they reported its unique ability to selectively bind glioma cells but not healthy tissue. This affinity for glioma increases in proportion to the grade of the tumor, with chlorotoxin binding 100% of grade IV glioma (GBM) cells (31/31 samples positive) [18]. Importantly, chlorotoxin also displayed high selectivity for GBM, as it was found to not bind samples of various healthy human tissues. Together, these qualities make the peptide an interesting candidate for use in GBM treatment.

Owing to its selectivity for glioma cells and lack of toxicity to humans, chlorotoxin has found relevance as a supplementary tool within the current standard of care. In the clinical setting, a modified chlorotoxin molecule attached to a Cy5.5 infrared dye, coined Tumor Paint, has been utilized to enhance visualization of the tumor during surgery in mice and is awaiting clinical trials in humans [19]. Despite intensive research and promising clinical applications, chlorotoxin's binding target on glioma cells remains unknown. Multiple potential targets have been reported, including matrix metalloproteinase 2 (MMP-2), annexin A2, Nrp1, and glioma-specific chloride channels, yet none have demonstrated evidence of direct interaction with chlorotoxin [20-23]. Regardless, it is clear that chlorotoxin possesses incredible therapeutic potential as a targeting molecule for GBM.

1.5 *ACDClxΔ15*

Prior work by Rebecca Cook utilized the unique glioma-binding specificity of chlorotoxin to design a fusion protein immunotherapy resembling a modified BiTE molecule. Named anti-CD3/chlorotoxin (ACDClx), this construct tethered chlorotoxin to the V_H/V_L scFv of a mouse anti-CD3ε monoclonal antibody (mAb) (2C11). ACDClx was

designed to bring T cells into contact with GBM in order to initiate perforin/granzyme-mediate apoptosis of tumor cells, with the specificity to eliminate all GBM cells and the selectivity to prevent off-target toxicity against healthy cells. Despite promising preliminary results *in vitro*, recombinant production of ACDClx in *Nicotiana benthamiana* and *Escherichia coli* expression systems was marred by improper folding of chlorotoxin during translation and purification steps, likely owing to its intricate structure. Eight of chlorotoxin's 36 amino acids are cysteine residues, which form four disulfide bonds (DSBs) in a highly compact inhibitor-cysteine knot (ISK) motif [24]. These DSBs posed problems during the expression of ACDClx in both *N. benthamiana* and *E. coli*, as in both systems DSB formation outside of its natural context resulted in largely insoluble, aggregated protein. In *E. coli*, DSB formation during recombinant expression has been previously achieved by selectively expressing the gene of interest within the periplasm [25]; however, periplasm targeted ACDClx remained insoluble in solution. Recently, researchers studying chlorotoxin as part of a peptide-drug conjugate (PDC) reported that chlorotoxin was metabolized in the GBM tumor microenvironment to form peptide fragments that retained their GBM-binding capabilities [22]. Interestingly, it appears that these fragments all retained a C-terminal arginine residue thought to be responsible for GBM binding. Using this information, the design of ACDClx was modified by the deletion of 22 amino acids from the C-terminus of chlorotoxin to create a new fusion protein, ACDClxΔ15 (Figure 1). This deletion reduces the number of cysteine residues present within the peptide from eight to two, thereby allowing for the formation of only one possible DSB within the truncated chlorotoxin molecule. Reduction of DSB formation is theorized to allow for more efficient production of ACDClxΔ15 while still retaining its ability to bind GBM cells.

1.6 *Study aims*

The aim of this study was to effectively produce ACDClxΔ15 and analyze its functional capabilities as a potential treatment candidate for GBM. Specifically, this study aims to demonstrate the ability of ACDClxΔ15 to bind GBM and T cells in mice as well as induce selective T cell activation against mouse GBM cells *in vitro*. Production of ACDClxΔ15 in an *E. coli* expression system was verified by Western blot analysis and purified ACDClxΔ15 was tested for its functional capabilities via immunocytochemistry (ICC), flow cytometry and fluorescence-activated cell sorting (FACS).

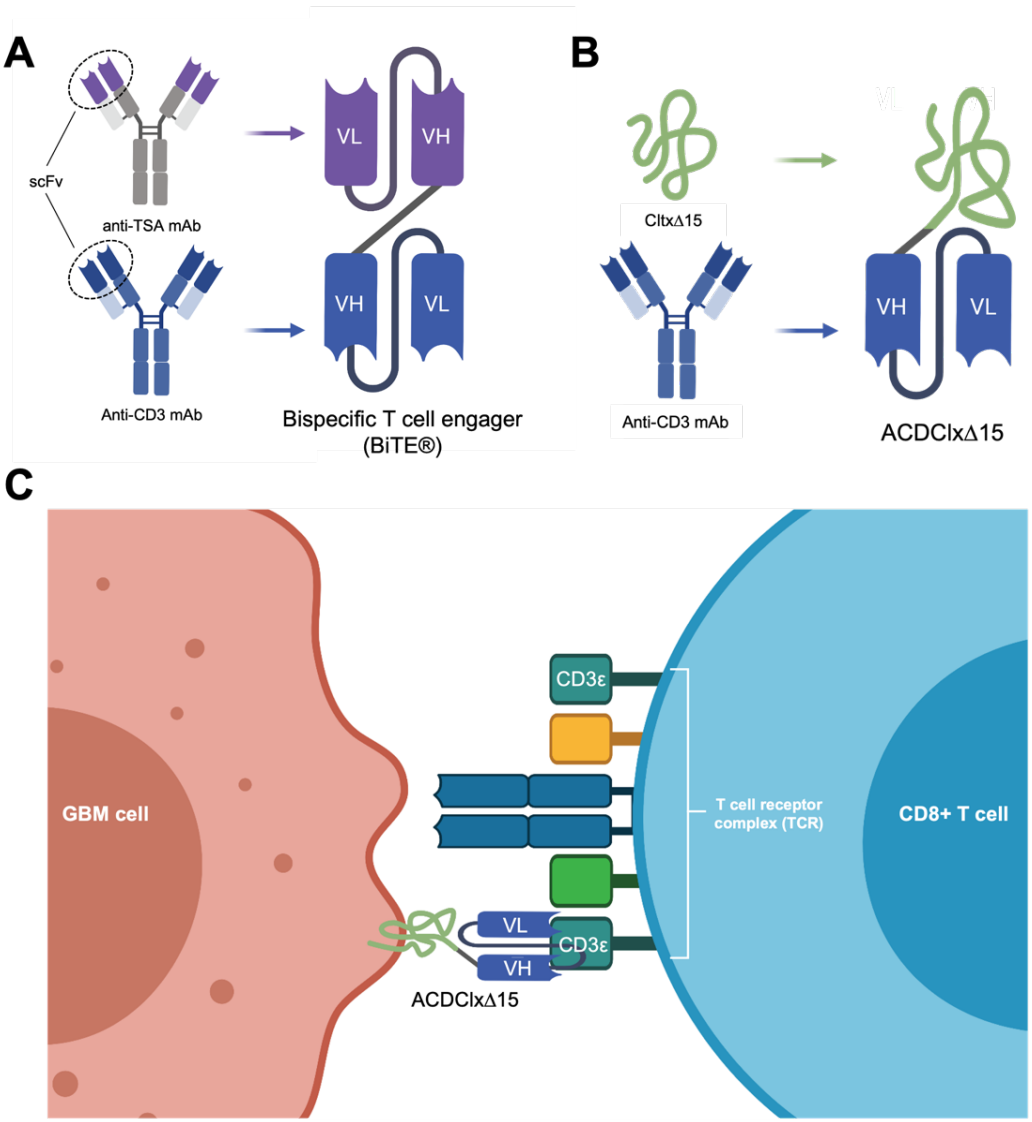

Figure 1. Fusion protein designs and interaction with target cells. Schematic depictions of BiTE® (A) and ACDClxΔ15 (B) models. scFv = single-chain variable fragment, TSA = tumor-specific antigen, mAb = monoclonal antibody, CltxΔ15 = truncated chlorotoxin. (C) Schematic of interaction between CD8+ T cells and GBM cells resulting from targeted binding by ACDClxΔ15. Created with BioRender.com.

2. METHODS

2.1 *Design and production of ACDClxΔ15*

Table 1. Amino acid sequences of relevance to ACDClxΔ15

	Amino acid sequence
Mouse anti-CD3ε V_H (2C11):	EVQLVESGGGLVQPGKSLKLSCEASGFTFSGYGMHWVRQA PGRGLESVAYITSSSINIKYADAVKGRFTVSRDNAKNLLFLQ MNILKSEDTAMYYCARFDWDKNYWGQGTMVTVSS
Mouse anti-CD3ε V_L (2C11):	QMTQSPSSLPASLGDRVTINCQASQDISNYLNWYQQKPGKA PKLLIYYTNKLADGVPSRFSGSGSGRDSSFTISSLESEDIGSY YCQQYYNYPWTFGPGTKLEIKR
Chlorotoxin (Cltx):	MCMPCFTTDHQMARKCDDCCGGKGRGK
CltxΔ15:	MCMPCFTTDHQMAR

The amino acid sequence of ACDClxΔ15 was composed from previously published sequences of the V_H and V_L scFvs of the mouse anti-CD3ε mAb 2C11 and a truncated chlorotoxin molecule which was obtained through deletion of 22 amino acids from the C-terminus of full-length chlorotoxin (Table 1). These sequences were joined by a $(Gly_4Ser)_3$ linker and an 8x histidine tag (His-tag) was included at the N-terminus. The gene encoding ACDClxΔ15 was cloned into an ampicillin resistant pET-11a plasmid, and the resulting vector (pTM1031) was used to transform electrocompetent BL21 (DE3) *E. coli* cells by electroporation. Transformed cells recovered in SOC medium (CSH Protocols, 2006) for 1 hr at 37°C before growing overnight on agar plates treated with ampicillin. Antibiotic selection and PCR screening confirmed cell colonies positive for pTM1031; positive colonies were then grown in 1 L cultures and induced with 0.3 mM IPTG after 4 hrs of shaking. Cultures were then centrifuged at 6000 xg and 4°C for 20 min (Beckman JA-17 rotor #369691). Pelleted cells were resuspended in extraction buffer (150 mM NaCl, 50 mM Tris pH 8, and 2 mM EDTA in PBS) and freeze-thawed

twice to lyse cells. Resuspended cells were vortexed and incubated at 30°C on a shaker before adding 0.5% PMSF and 20 mg lysozyme. In 45 min increments, the following were added: 0.5% Triton X-100, followed by 0.18% DNAse I and 1 M $MgSO_4$. Samples receiving s-sulfonation to prevent DSB formation were denatured and s-sulfonated overnight at 4°C in buffer containing 6 M guanidine, 200 mM sodium sulfite, 150 mM sodium tetrathionate dihydrate, 50 mM Tris pH 8, and 150 mM NaCl. All samples were purified via metal-affinity chromatography by incubating overnight at 4°C with Roche cOmplete nickel affinity resin. Purified protein was eluted through the addition of 1 M imidazole to the column. Concentration of the resulting eluent was measured on an ND-1000 NanoDrop spectrophotometer. S-sulfonated samples were then refolded by diluting 1:100 v/v overnight at 4°C in oxidizing buffer (0.5 M arginine, 2 mM oxidized glutathione, 100 mM Tris base, and 2 mM EDTA in PBS). Samples were re-concentrated by centrifugation in Millipore Amicon Ultra-15 centrifugal filter tubes with a 3.5 kDa MW cutoff (GE Healthcare, Pittsburgh, PA) for 15 min at 4°C in a Beckman-Coulter JS-5.3 swinging-bucket rotor before being exchanged into PBS on a Sephadex G-25 desalting column. Mock-purified protein refers to samples collected from BL21 (DE3) *E. coli* cells that were not transformed with the pTM1031 plasmid. These samples were treated identically to those produced from transformed cells as described above.

2.2 *SDS-PAGE and Immunoblotting*

To verify the presence and purity of ACDClxΔ15 following purification, samples were mixed with 6x Laemmli buffer (4% SDS, 20% glycerol, 0.004% bromophenol blue, 0.125 M Tris-HCl, and 10% DTT in ddH_2O), boiled for 5 min at 100°C and briefly centrifuged before loading onto 4-20% Mini-PROTEAN TGX stain-free polyacrylamide gels (Bio-Rad) alongside Bio-Rad Precision Plus dual-color protein standards. Gels were run at 150 V for 40 min, or until the sample buffer reached the bottom of the gel.

Following SDS-PAGE, gels were imaged for total protein via UV transillumination before being transferred to nitrocellulose membranes on a Trans-Blot® SD semi-dry transfer cell at 15 V for 15 min. Membranes were blocked in PBST + 2.5% non-fat milk (PBST-M) solution for 1 hr at RT and washed with PBST for 15 min before staining with mouse anti-His primary Ab (Sigma H1029) for 30 min. Membranes were again washed with PBST for 15 mins before donkey anti-mouse HRP secondary Ab (Jackson ImmunoResearch #715-305-150) for 30 min. Following a final 15 min wash in PBST, membranes were incubated with HRP substrate for 1 min and exposed onto X-ray film for 30 sec in the dark.

2.3 *Immunocytochemistry*

GL261-LucNeo mouse glioblastoma cells and NIH-3T3 mouse embryonic fibroblasts (ATCC), generously provided by Dr. Adrienne C. Scheck at Barrow Neurological Institute and Dr. Debra P. Baluch at Arizona State University, respectively, were grown in culture media (DMEM + 10% FBS/F12 + 1% PSG) at 37°C to approximately 70% confluency. Cells were passaged and split 1:6 before seeding on four coverslips per cell line in separate wells of two 6-well plates. Cells were grown to approximately 90% confluency on coverslips before fixing in 1 mL 2% paraformaldehyde. Coverslips were washed with 1 mL PBS + 5% nonfat milk (PBS-M) before adding 1 mL of 1 μM ACDClxΔ15 in PBS for 1 hr on the rocker at 4°C. Cells were washed with 1 mL PBS-M 3x for 5 min each on a rocker at RT. Mouse anti-6xHis primary antibody was added to all coverslips except secondary control at a 1:500 dilution in 1 mL PBS-M and incubated on rocker at 4°C overnight. Primary antibody was removed before adding 1 mL of secondary antibody (donkey anti-mouse IgG H&L Alexa Fluor® 488, Abcam ab150109) and incubating in the dark at 4°C on a rocker for 1 hr. Secondary antibody was removed and coverslips were washed with PBS-M 3x for 5 min each on rocker. Antibody wash was

removed, and cells were incubated with DAPI nuclear stain for 30 min before mounting and sealing coverslips on microscope slides. Slides were imaged on a Leica SP8 White Light Laser Confocal microscope using a 488 nm wavelength laser.

2.4 *Analyzing GBM binding via Flow Cytometry*

GL261-LucNeo cells were grown in culture media (DMEM + 10% FBS + 1% pen/strep) to approximately 90% confluency. Cells were harvested and washed with FACS buffer (1% bovine serum albumin and 0.1% sodium azide in PBS) and aliquoted into a 96-well round bottom plate (approx. $1.0x10^6$ cells/well). Cells were washed 2x with FACS buffer by centrifugation for 5 min at 1200 rpm on a Thermoscientific Bioliner rotor (#75003667) before being incubated with either 5 μM ACDClxΔ15, mock-purified protein, or PBS for 30 min at 4°C. Anti-6xHis-PE antibody was added to all samples except one PBS-only control at a 1:200 dilution in FACS buffer and incubated for 30 min at 4°C. Samples were again washed as before and resuspended in 1 mL FACS buffer before running on a BD LSRFortessa™ flow cytometer. Results were analyzed using FlowJo™ v10.8 software (BD Life Sciences).

2.5 *Analyzing GBM-T cell interactions via Flow Cytometry and FACS*

Table 2. Fluorescent antibodies used for flow cytometry and FACS experiments

Antibody	Fluorophore	Catalog #
anti-6xHis	APC	362605 (BioLegend)
anti-beta tubulin	Alexa Fluor® 488	A4-251-C100 (EXBIO)
anti-CD4	V450	FP20224002 (MBL International)
anti-CD8a	Brilliant Violet 711	100747 (BioLegend)
anti-CD69	PE-Dazzle 594	104535 (BioLegend)

GL261-LucNeo cells were grown and prepared for flow cytometry as described in Section 2.4 and aliquoted into 15 mL Falcon™ tubes. Spleens were harvested from wild-type mice and splenocytes were isolated by straining spleens into RPMI media. Red blood cells were lysed by centrifugation for 5 min at 1200 rpm and 4°C before incubating in 1 mL Ack Lysis buffer for 2 min at RT. Cells were quenched with RPMI and centrifuged as above before resuspending in 8 mL final volume of RPMI on ice. Splenocytes were counted and approximately $1.0x10^6$ cells were aliquoted into separate Falcon™ tubes and incubated with their respective treatments. Antibodies used in this experiment are listed in Table 2**,** and 1 mL ACDClxΔ15 was added to samples at 1 μM concentration. All incubations were performed for 30 min at 4°C in the dark except for anti-CD69, which was incubated for 2 hrs. Two washes were performed between each incubation by centrifuging samples at 1200 rpm for 5 min at 4°C and resuspending cells in 2 mL FACS buffer. Following the final wash, samples were resuspended in 1 mL FACS buffer and collected on a ThermoFischer Attune NxT flow cytometer before analyzing as described in Section 2.4.

2.6 *Cell sorting*

Samples obtained in Section 1.4 were run on a BD FACSAria™ IIu cell sorter in order to identify samples positive for both GBM and T cells. Samples in which GBM and splenocytes were co-incubated with ACDClxΔ15 and all five antibodies were sorted for events that were positive for anti-6xHis and either anti-CD4 or anti-CD8 to indicate GBM-T cell binding events. Resulting samples were plated onto coverslips and fixed before imaging on a Lecia SP8 confocal microscope.

3. RESULTS

3.1 *Design and production of ACDClxΔ15 in E. coli*

In order to produce ACDClxΔ15, the gene encoding its components was cloned into a plasmid capable of transforming electrocompetent *E. coli* cells (Figure 2A). Following induction with IPTG, cells were harvested and ACDClxΔ15 was present in insoluble inclusion bodies within the total cell lysate of transformed cells but not in untransformed cells, as detected by Western blot (Figure 2B). Purification and subsequent concentration resulted in a 24% yield of ACDClxΔ15 (Figure 2C). Any proteins present in untransformed samples (mock-purified protein) were not detected by anti-His antibody and therefore were not expected to be capable of binding nickel resin for purification.

3.2 *Analyzing ACDClxΔ15-GBM binding in vitro*

For the first test of CltxΔ15's ability to bind GBM cells as part of a BiTE-like molecule, ACDClxΔ15 was incubated with GL261-LucNeo mouse glioblastoma cells and stained with antibodies which fluoresce when excited with lasers at a wavelength of 488 nm. When incubated with ACDClxΔ15 and visualized with fluorescent confocal microscopy, GBM cells displayed bright green fluorescence compared to mouse embryonic fibroblast cells (NIH-3T3) also incubated with ACDClxΔ15 (Figure 3A, B). Control samples receiving either mock protein, primary and secondary Ab only, or ACDClxΔ15 and secondary Ab alone displayed negligible levels of fluorescence (Figure 3C,D).

As a quantitative method to measure ACDClxΔ15-GBM binding, GL261-LucNeo cells were incubated with PBS, mock protein, anti-6xHis-PE, or ACDClxΔ15 and analyzed using flow cytometry. A distinct peak was observed for samples treated with ACDClxΔ15 but not those receiving controls (Figure 4A). Dot plots of all events recorded

per sample showed similar results, with clear increases in cells positive for anti-6xHis-PE observed compared to controls (Figure 4B). After gating for positive cells based on these negative controls, the percent of positive cells was calculated and found to be higher in samples treated with ACDClxΔ15, with 35.5% of cells displaying fluorescence compared to 0.92%, 0.59%, and 0.59% for samples treated with PBS, anti-6xHis, and mock protein respectively (Figure 4C). Median fluorescent intensity of positive events was likewise higher in ACDClxΔ15 samples than in controls (Figure 4D). Together, these results indicate that ACDClxΔ15 is capable of binding murine GBM cells, but not other mouse tissue types, *in vitro*.

3.3 *GBM-T cell binding and activation in vitro*

After testing its ability to bind mouse GBM cells specifically via fluorescence microscopy and flow cytometry, ACDClxΔ15 was then co-incubated with GBM cells and splenocytes to determine whether or not it was capable of both binding and activating T cells in the presence of GBM. To achieve this, flow cytometry was again utilized to measure fluorescent signals of co-incubated GBM and T cells treated with specific antibodies that would detect the presence of important markers of T cell binding and activation. Specifically, T cells were stained for the presence of CD4 and CD8 and incubated with GBM cells stained for beta tubulin and binding events were determined by the presence of GBM and either CD4 or CD8 probes in single recorded events. As expected, samples of GBM and T cells co-incubated with or without ACDClxΔ15 displayed prominent peaks when probed with anti-beta tubulin, anti-CD4, and anti-CD8, which act as markers for these cells (Figure 5A). The sample which received ACDClxΔ15 showed a small signal peak for its corresponding anti-His detection while all other samples displayed negligible fluorescence.

Following flow cytometry, cells were sorted using FACS to isolate events that contained GBM cells, CD8+ T cells, and ACDClxΔ15. These samples were imaged using confocal microscopy in order to visualize binding events between GBM and T cells (Figure 5C). Fluorescence was detected for all three probed antibodies, and a CD8+ cell was observed in close proximity to a cell positive for anti-beta tubulin, the marker used here to identify GBM cells. However, isolated scans show that this anti-beta tubulin signal was also present on the CD8+ cell.

To measure T cell activation in the presence of GBM, Early T cell activation antigen (CD69) was also probed following co-incubation of GBM and T cells for 2 hours. Samples of GBM cells incubated with T cells displayed very slight positive deviations from all other samples when probed for CD69 expression (Figure 5A). Within samples of GBM and T cells incubated either with or without ACDClxΔ15, populations of cells were found to be positive for both GBM and CD4/CD8, signifying potential binding events (Figure 5B). Of these samples, cells treated with ACDClxΔ15 displayed more distinct populations of double-positive cells than untreated cells. These results would indicate that while ACDClxΔ15 is capable of binding T cells, there is little evidence to suggest it is able to activate T cells in the presence of GBM.

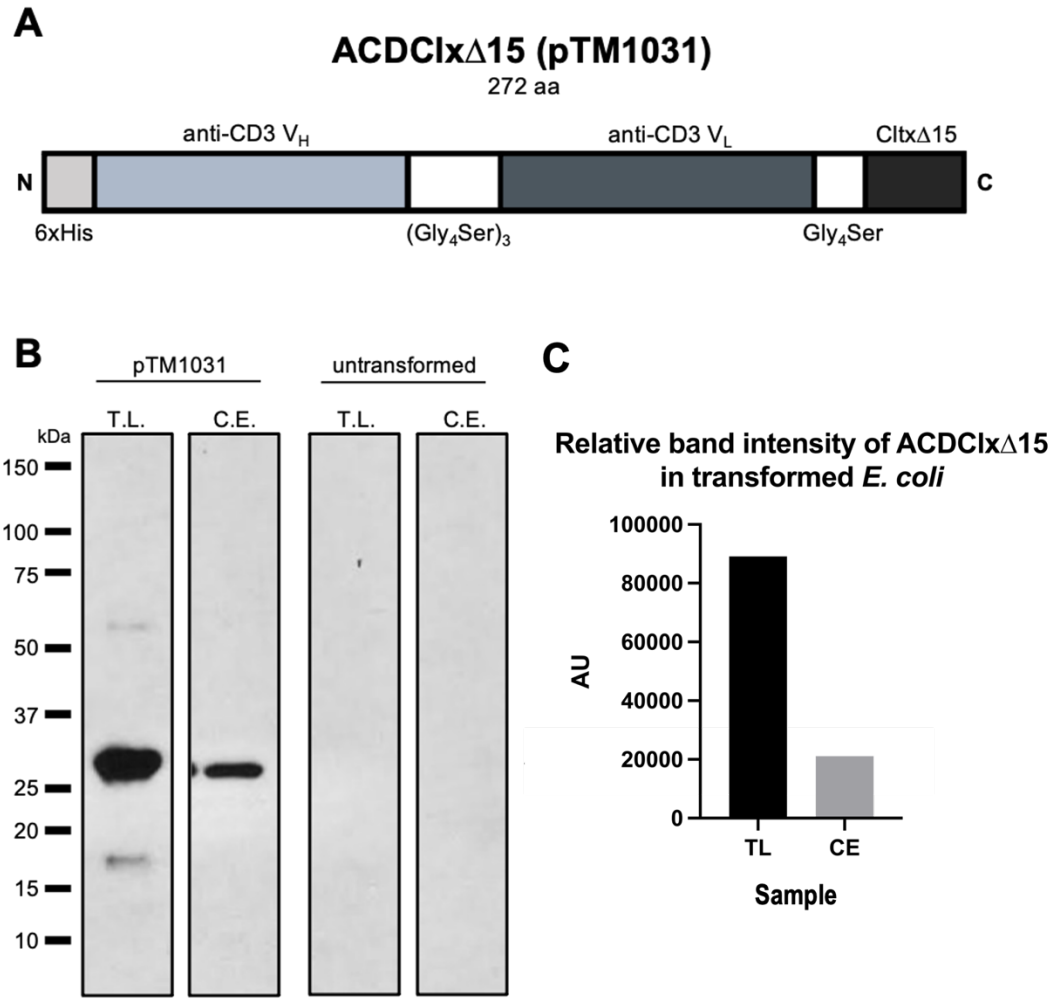

Figure 2. Design and expression of ACDClxΔ15 in *E. coli*. (A) Gene map showing design of ACDClxΔ15. N/C refer to N- and C-terminus of protein product. (B) Western blot verifying presence of ACDClxΔ15 in *E. coli* inclusion body samples derived from cells transformed with pTM1031 compared to untransformed cells. TL = total lysate, CE = concentrated elution. (C) Graph depicting band intensity of ACDClxΔ15 detected by Western blot for both samples. AU = arbitrary units. Expected MW of ACDClxΔ15 = 28.7 kDa

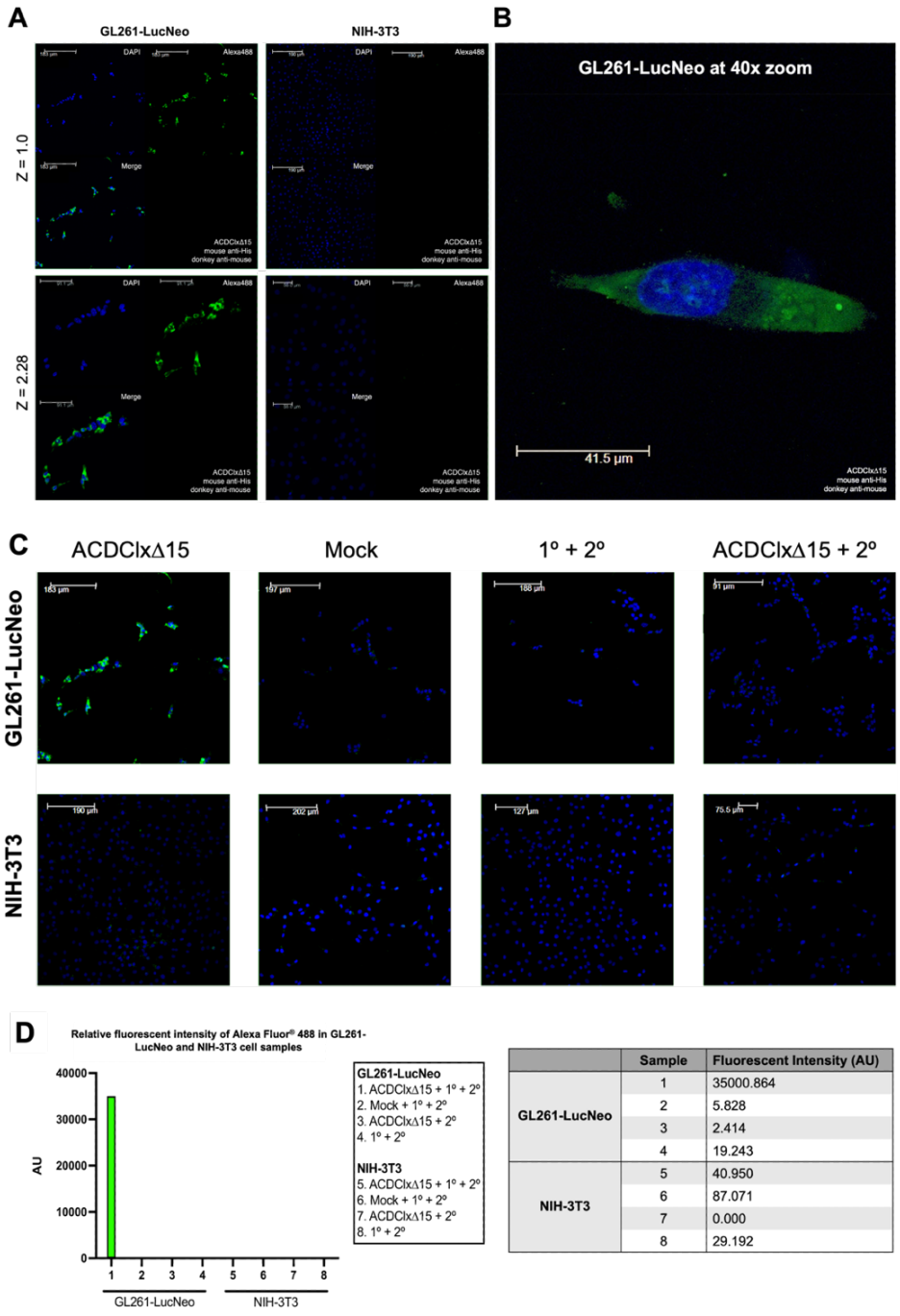

	Sample	Fluorescent Intensity (AU)
GL261-LucNeo	1	35000.864
	2	5.828
	3	2.414
	4	19.243
NIH-3T3	5	40.950
	6	87.071
	7	0.000
	8	29.192

Figure 3. Analysis of GBM binding via immunocytochemistry. (A) Comparison of GBM and NIH-3T3 cells incubated with ACDClxΔ15. Images were obtained by fluorescent microscopy at two objectives (zoom = 1.0, zoom = 2.28). Green = donkey anti-mouse Alexa Fluor® 488, blue = DAPI nuclear stain. (B) 40x zoom of GBM cell incubated with ACDClxΔ15 and DAPI nuclear stain. (C) Comparison of all samples including controls between NIH-3T3 and GL261-LucNeo cells. 1° = primary Ab, 2° = secondary Ab. (D) Bar graph and table depicting relative levels of Alexa Fluor® 488 across all samples, measured in arbitrary units (AU).

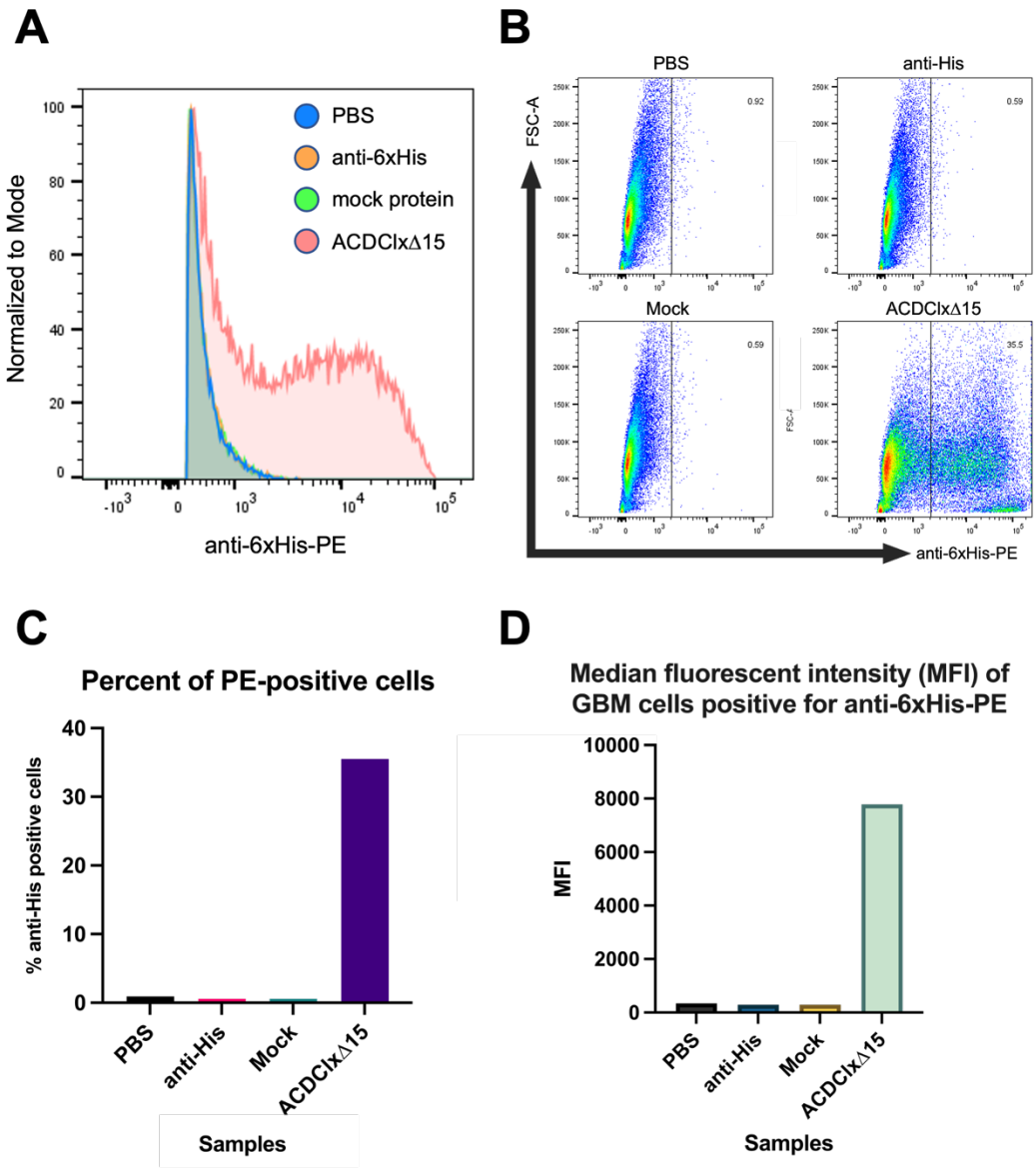

Figure 4. Analysis of ACDClxΔ15-GBM binding via flow cytometry. Histogram (A) and dot plots (B) displaying detected fluorescence of GL261-LucNeo cells incubated with PBS, anti-6xHis-PE, mock protein, or ACDClxΔ15 for PE. Negative controls were used to gate for positive events. Bar graphs displaying number of PE-positive events (C) and median fluorescent intensity (MFI) (D) for each sample.

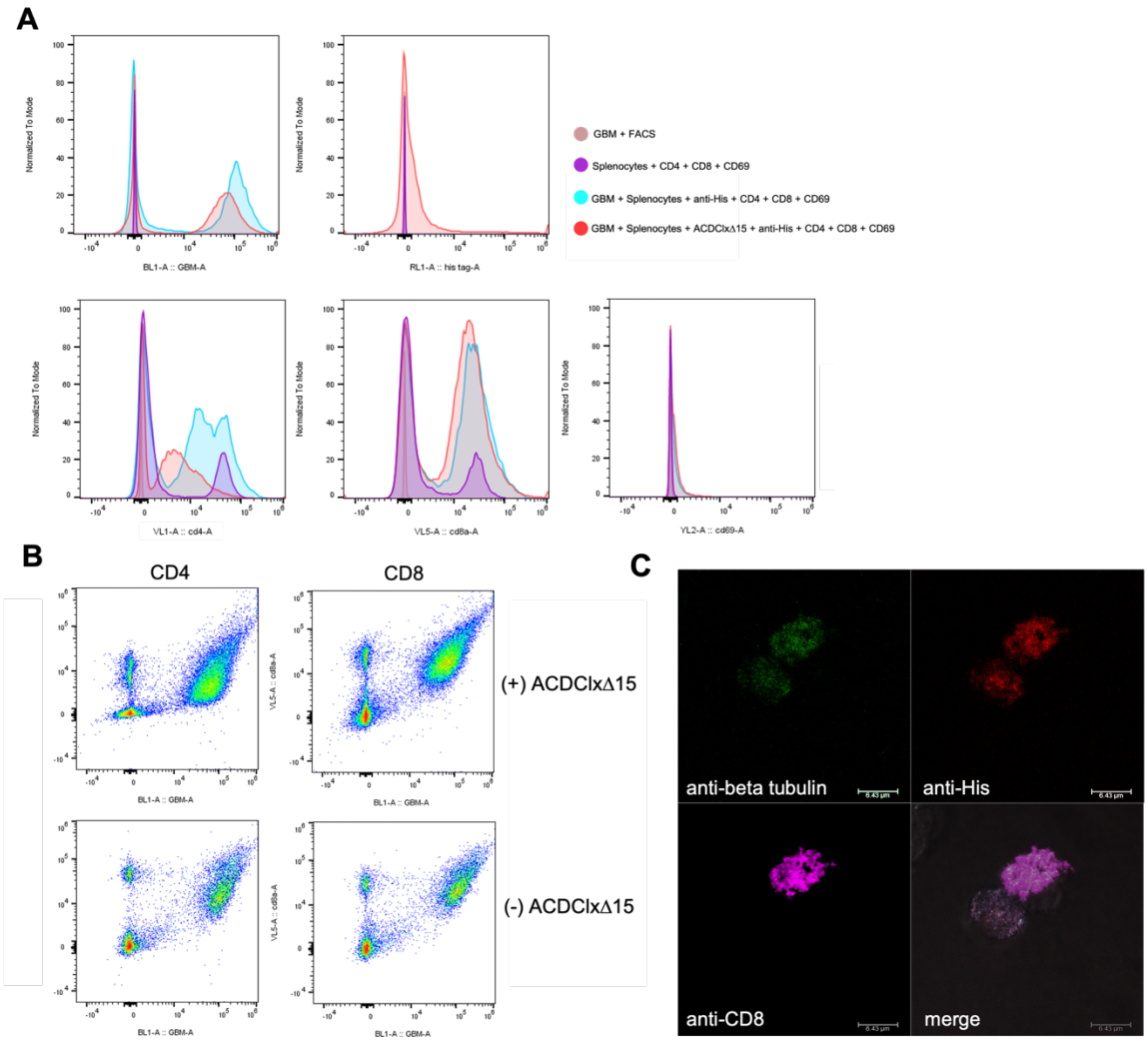

Figure 5. Analysis of GBM-T cell interactions via flow cytometry and FACS. (A) Histograms showing levels of fluorescence detected across cell samples incubated with various treatments (see legend). Each histogram is specific to one fluorophore: anti-beta tubulin, anti-His, anti-CD4, anti-CD8a, and anti-CD69. FACS buffer was used to incubate cells as a control for autofluorescence. (B) Dot plots measuring co-fluorescence of cells for GBM (x-axis) and either CD4+ or CD8+ T cells (y-axis) in samples either with or without ACDClxΔ15. (C) Confocal microscopy of cells sorted for presence of anti-beta tubulin, anti-His, and anti-CD8a.

4. DISCUSSION

Immunotherapies such as the bispecific T cell engager represent the most promising of new, experimental treatment strategies for glioblastoma in part due to their unique ability to stimulate T cell responses against cancer. Although capable of surpassing many of the hurdles standing in the way of effective GBM treatment, these immunotherapies have been largely ineffective due to the lack of a universal target for GBM. Chlorotoxin, a scorpion-derived peptide, has been shown to overcome this through its unique ability to bind human glioma cells without off-target toxicity to other tissues. I hypothesized that a fusion protein immunotherapy in the design of a modified BiTE which utilizes a modified chlorotoxin peptide to target GBM cells could be capable of bringing GBM into contact with, and subsequently activating, T cells. My findings demonstrate that while a BiTE-like molecule utilizing a truncated chlorotoxin molecule retains its ability to bind GBM cells as well as T cells, it is unable to induce T cell activation as measured here. This study nevertheless confirms the hypothesis that peptide fragments resulting from the uptake of chlorotoxin in human glioma cells retain their ability to bind GBM cells, likely due to the presence of a C-terminal arginine residue.

The goal of this study was threefold: (1) to produce a recombinant fusion protein immunotherapy for glioblastoma using a truncated chlorotoxin molecule to target GBM (ACDClxΔ15), (2) to determine this protein's ability to bind GBM and T cells, and (3) analyze whether it is capable of activating T cells against GBM. ACDClxΔ15 was produced by transformed *E. coli* cells in the form of inclusion bodies and purified via metal affinity chromatography (Figure 2B). Following purification, ACDClxΔ15 was successfully transferred to PBS buffer to be used for *in vitro* experiments while maintaining solubility. However, a significant fraction of ACDClxΔ15 present initially in

total cell lysates was lost during the purification process (approx. 75%). While the total yield was sufficient for the present study, it is worth investigating potential causes for this loss of protein in order to more efficiently produce ACDClxΔ15 moving forward.

In response to reports of truncated chlorotoxin fragments retaining their GBM-binding abilities, I examined the ability of one such peptide, CltxΔ15, to bind GL261-LucNeo mouse GBM cells selectively. To first test this, GBM cells and NIH-3T3 mouse embryonic fibroblast cells were incubated with ACDClxΔ15, which was then probed for its N-terminal histidine-tag with fluorescent antibodies. Confocal microscopy of these samples revealed that ACDClxΔ15 did bind GBM cells but did not bind healthy fibroblast cells (Figure 3). These results were verified using flow cytometry to measure the number of cells that were positive for ACDClxΔ15 in much the same way as the previous imaging experiment. As expected, ACDClxΔ15 further demonstrated its ability to bind GBM cells *in vitro*, with high levels of fluorescence detected for anti-6xHis-PE among cells incubated with ACDClxΔ15 when compared to control samples (Figure 4). Together, these results confirmed my hypothesis that CltxΔ15 is capable of selectively binding GBM cells without off-target toxicity when part of a BiTE-like fusion protein.

Finally, this study aimed to examine whether or not ACDClxΔ15 is capable of binding and activating T cells against GBM cells *in vitro*. Flow cytometry was again utilized to detect the presence of T cells (CD4, CD8), GBM cells (beta tubulin), and ACDClxΔ15 (His-tag), as well as a marker for the activation of T cells (CD69). In samples of GBM and T cells incubated with ACDClxΔ15, strong co-expression of beta tubulin and either CD4 or CD8 was observed, possibly indicating that these events were measured as a GBM-T cell doublet (Figure 5). However, this phenomenon was also observed to a lesser degree in samples of GBM and T cells that were not incubated with ACDClxΔ15, casting uncertainty over the ability of ACDClxΔ15 to bring GBM and T cells together.

When sorted via fluorescence-activated cell sorting (FACS) and imaged for their fluorescent antibody probes, individual events that showed positive signals for ACDClx, CD8a, and anti-beta tubulin (GBM) were able to be isolated and imaged using confocal microscopy. In these images, CD8+ T cells and GBM cells were observed to be forming a cell doublet, and isolated images of each fluorescent probe showed strong signal for ACDClxΔ15 on the CD8+ cell, indicating that ACDClxΔ15 is capable of binding T cells. However, anti-beta tubulin signal was also detected on the same cell, posing a problem in drawing any conclusions about ACDClxΔ15-T cell binding. This phenomenon could also explain the observation of events positive for both GBM and either CD4 or CD8 within the prior flow cytometry experiment. Due to the lack of known GBM-specific binding targets capable of being used as fluorescent probes outside of chlorotoxin and its various fragmented peptide products, anti-beta tubulin was used to label these cells, which were treated with Tubulin Tracker™ prior to staining. This dye is known to easily permeate cell membranes in live cells, which often leads to unwanted bleeding of stain between co-incubated cells. This likely explains the double-positive cells observed; however, of the two cells observed by imaging of sorted events, one was only positive for anti-beta tubulin alone, while the other was positive for both anti-beta tubulin and CD8. This may well indicate that these two cells were in fact a GBM cell and a separate CD8+ T cell, which would support the conclusion that ACDClxΔ15 is capable of binding T cells due to the aforementioned anti-His signal observed coating the CD8+ cell. Unfortunately, these results lacked any convincing evidence of potential T cell activating abilities of ACDClxΔ15, as only minor deviations in CD69 expression were detected among both of these samples (Figure 5A).

Although the results of this study successfully demonstrate that ACDClxΔ15 is capable of binding mouse GBM cells *in vitro*, its ability to bind and activate T cells

remains unclear. Future work will aim to clarify these questions by utilizing various other techniques to measure T cell binding and activation. Specifically, T cells will be subjected to imaging via immunocytochemistry in the same way as GL261-LucNeo cells were in order to visually isolate and identify the presence of ACDClxΔ15 in these cell samples. Finally, more immediate markers of T cell activation, such as detection of calcium flux, will be used to supplement CD69 expression, which will be measured following a longer incubation with ACDClxΔ15. Overall, this study acts as yet another step towards improving and enhancing the current, outdated standard of care for treatment of GBM while expanding the burgeoning field of cancer immunotherapy.

REFERENCES

1. Louis DN, Ohgaki H, Wiestler OD, et al. (2007). The 2007 WHO Classification of Tumours of the Central Nervous System. *Acta Neuropathologica,* 114(2):97-109.

2. Ostrom QT, Gittleman H, Liao P, et al. (2014). CBTRUS statistical report: primary brain and central nervous system tumors diagnosed in the United States in 2007-2011. *Neuro Oncol,* 16 Suppl 4:iv1-63.

3. Yung WKA, Horten BC, Shapiro WR. (1980). Meningeal gliomatosis: A review of 12 cases. *Ann Neurol* 8:605–608.

4. Gallego, O. (2015). Nonsurgical treatment of recurrent glioblastoma. *Current Oncology*, *22*(4), e273–e281.

5. Stupp, Roger et al. (2009). Effects of radiotherapy with concomitant and adjuvant temozolomide versus radiotherapy alone on survival in glioblastoma in a randomised phase III study: 5-year analysis of the EORTC-NCIC trial. *The Lancet Oncology*, Volume 10, Issue 5, 459–466.

6. Annovazzi, L., Mellai, M., & Schiffer, D. (2017). Chemotherapeutic Drugs: DNA Damage and Repair in Glioblastoma. *Cancers*, *9*(6), 57.

7. W.M. Pardridge (2005). The blood-brain barrier: bottleneck in brain drug development*, NeuroRx J. Am. Soc. Exp. Neurother*. 3–14.

8. Mason WP, Mirimanoff RO, Stupp R (2006). Radiotherapy with Concurrent and Adjuvant Temozolomide: A New Standard of Care for Glioblastoma Multiforme. *Progress in Neurotherapeutics and Neuropsychopharmacology*. 1. pp. 37–52.

9. V.F. Zhu, J. Yang, D.G. Lebrun, M. Li. (2012). Understanding the role of cytokines in Glioblastoma Multiforme pathogenesis*, Cancer Lett*. 316:139–150.

10. M.-L. Chen, M.J. Pittet, L. Gorelik, R.A. Flavell, R. Weissleder, H. von Boehmer, K. Khazaie. (2005). Regulatory T cells suppress tumor-specific CD8 T cell cytotoxicity through TGF-beta signals in vivo*, Proc. Natl. Acad. Sci. U. S. A.* 102:419–424.

11. D. Zagzag, K. Salnikow, L. Chiriboga, H. Yee, L. Lan, M.A. Ali, R. Garcia, S. Demaria, E.W. Newcomb. (2005). Downregulation of major histocompatibility complex antigens in invading glioma cells: stealth invasion of the brain*, Lab. Investig. J. Tech. Methods Pathol.* 85:328–341.

12. Grossman, S. A., Ye, X., Lesser, G., Sloan, A., Carraway, H., Desideri, S., Piantadosi, S., & NABTT CNS Consortium (2011). Immunosuppression in patients with high-grade gliomas treated with radiation and

temozolomide. *Clinical cancer research : an official journal of the American Association for Cancer Research*, *17*(16), 5473–5480.

13. An, Z., Aksoy, O., Zheng, T. *et al.* (2018). Epidermal growth factor receptor and EGFRvIII in glioblastoma: signaling pathways and targeted therapies. *Oncogene* 37**,** 1561–1575.

14. D.A. Reardon, J. Schuster, D.D. Tran, K.L. Fink, L.B. Nabors, G. Li, D.A. Bota, R.V. Lukas, A. Desjardins, L.S. Ashby, J.P. Duic, M.M. Mrugala, A. Werner, T. Hawthorne, Y. He, J.A. Green, M.J. Yellin, C.D. Turner, T.A. Davis, J.H. Sampson,(2015). ReACT: Overall survival from a randomized phase II study of rindopepimut (CDX-110) plus bevacizumab in relapsed glioblastoma., *J. Clin. Oncol.* 33 2009–2009.

15. P.A. Baeuerle, C. Reinhardt. (2009). Bispecific T-Cell Engaging Antibodies for Cancer Therapy, *Cancer Res.* 69:4941–4944.

16. B.D. Choi, P.C. Gedeon, J.E. Herndon, G.E. Archer, E.A. Reap, L. Sanchez-Perez, D.A. Mitchell, D.D. Bigner, J.H. Sampson. (2013). Human Regulatory T Cells Kill Tumor Cells through Granzyme-Dependent Cytotoxicity upon Retargeting with a Bispecific Antibody, *Cancer Immunol.* Res. 1:163–167.

17. P.C. Gedeon, T.H. Schaller, S.K. Chitneni, B.D. Choi, C.-T. Kuan, C.M. Suryadevara, D.J. Snyder, R.J. Schmittling, S.E. Szafranski, X. Cui, P. Healy, J.E. Herndon, R.E. McLendon, S.T. Keir, G.E. Archer, E. Reap, L. Sanchez-Perez, D.D. Bigner, J.H. Sampson. (2018). A rationally designed fully human EGFRvIII:CD3-targeted bispecific antibody redirects human T cells to treat patient-derived intracerebral malignant glioma, *Clin. Cancer Res.* clincanres.0126.2017.

18. S.A. Lyons, J. O'Neal, H. Sontheimer. (2002). Chlorotoxin, a scorpion-derived peptide, specifically binds to gliomas and tumors of neuroectodermal origin, *Glia.* 39 162–173.

19. M. Veiseh, P. Gabikian, S.-B. Bahrami, O. Veiseh, M. Zhang, R.C. Hackman, A.C. Ravanpay, M.R. Stroud, Y. Kusuma, S.J. Hansen, D. Kwok, N.M. Munoz, R.W. Sze, W.M. Grady, N.M. Greenberg, R.G. Ellenbogen, J.M. Olson. (2007). Tumor Paint: A Chlorotoxin:Cy5.5 Bioconjugate for Intraoperative Visualization of Cancer Foci, *Cancer Res.* 67 6882–6888.

20. J. Deshane, C.C. Garner, H. Sontheimer. (2003). Chlorotoxin Inhibits Glioma Cell Invasion via Matrix Metalloproteinase-2, *J. Biol. Chem.* 278 4135–4144.

21. K. Kesavan, J. Ratliff, E.W. Johnson, W. Dahlberg, J.M. Asara, P. Misra, J.V. Frangioni, D.B. Jacoby. (2010). Annexin A2 Is a Molecular Target for TM601, a Peptide with Tumor-targeting and Anti-angiogenic Effects, *J. Biol. Chem.* 285 4366–4374.

22. D. Kolber-Simonds, J. Wu, U. Majumder, D. Custar, D. Li, H. Du, M.H. Postema, T. Noland, A. Hart, G. Lai, S. Eckley, V. Dixit, K. Tendyke, K. Nomoto, M. Woodall-Jappe, S. McGonigle. (2018). Abstract 3961: Role for neuropilin1 in mode of action of chlorotoxin, *Cancer Res*. 78 3961–3961.

23. N. Ullrich, A. Bordey, G.Y. Gillespie, H. Sontheimer. (1998) Expression of voltage-activated chloride currents in acute slices of human gliomas, *Neuroscience*. 83 1161–1173.

24. RCSB PDB - Protein Feature View - Chlorotoxin - P45639 (CTXL_LEIQU), (n.d.). http://www.rcsb.org/pdb/protein/P45639 (accessed October 12, 2021).

25. Gąciarz, A., Khatri, N.K., Velez-Suberbie, M.L. *et al.* (2017). Efficient soluble expression of disulfide bonded proteins in the cytoplasm of *Escherichia coli* in fed-batch fermentations on chemically defined minimal media. *Microb Cell Fact* 16, 108.